Annals of Nuclear Medicine (2019) 33:766–775
https://doi.org/10.1007/s12149-019-01387-0

ORIGINAL ARTICLE

68Ga-PSMA-11 PET/CT derived quantitative volumetric tumor parameters for classification and evaluation of therapeutic response of bone metastases in prostate cancer patients

Christian Schmidkonz[1,5] · Michael Cordes[1] · Theresa Ida Goetz[1,4] · Olaf Prante[1] · Torsten Kuwert[1] · Philipp Ritt[1] · Michael Uder[2] · Bernd Wullich[3] · Peter Goebell[3] · Tobias Bäuerle[2]

Received: 7 June 2019 / Accepted: 16 July 2019 / Published online: 23 July 2019

Abstract

Background To evaluate the role of ^{68}Gallium prostate-specific membrane antigen-positron emission tomography/computed tomography (^{68}Ga-PSMA-11 PET/CT) derived quantitative volumetric tumor parameters in comparison with fully diagnostic conventional CT and serum-PSA levels for classification and evaluation of therapeutic response of bone metastases in patients with metastasized prostate cancer (PC).

Methods A total of 177 men with biochemical recurrence of prostate cancer suffering from bone metastases underwent PET/CT with [^{68}Ga] Ga-PSMA-HBED-CC (^{68}Ga-PSMA-11). To calculate ^{68}Ga-PSMA-11 PET quantitative volumetric tumor parameters including whole-body total-lesion PSMA (TL-PSMA), whole-body PSMA-tumor volume (PSMA-TV), as well as the established maximum standard uptake values (SUVmax) and mean standard uptake values (SUVmean), all 443 ^{68}Ga-PSMA-11-positive bone lesions in the field of view were assessed quantitatively. Quantitative volumetric tumor parameters were correlated with CT-derived volume and bone density measurements of metastatic bone lesions, serum prostate-specific antigen (PSA) levels, and Gleason Scores. In the 20 patients suffering from bone metastases who underwent ^{68}Ga-PSMA-11 PET/CT before and after therapy, CT-derived volume and bone density measurements of metastatic lesions were compared to biochemical response determined by serum-PSA levels.

Results In 177 patients, a total of 443 ^{68}Ga-PSMA-11 PET-positive bone lesions were detected. Of these, 50 lesions (11%) were only detectable on PET but not on conventional CT. PET-positive/CT-negative bone metastases demonstrated a significantly lower PSMA uptake compared to PET-positive/CT-positive bone lesions ($p < 0.05$). SUVmax, SUVmean, PSMA-TV, and TL-PSMA of bone metastases were significantly higher ($p < 0.05$) in patients with Gleason Scores > 7 compared to those with Gleason Scores ≤ 7. In the linear regression analysis, an association was determined between SUVmean, Gleason Scores, lesion classification, and serum-PSA levels but not for CT-derived bone density measurements. No significant correlation could be found between changes of bone density and CT-derived volume measurements of metastatic bone lesions and changes of serum-PSA levels ($p > 0.05$) before and after therapy, while a highly significant correlation was observed for changes of PSMA-TV, TL-PSMA, and serum-PSA levels ($p < 0.001$).

Conclusion Our results suggest that ^{68}Ga-PSMA-11 PET/CT might be a valuable tool for the detection and follow-up of bone metastases in patients with metastasized prostate cancer. ^{68}Ga-PSMA-11 PET-derived quantitative volumetric parameters demonstrated a highly significant correlation with changes of serum-PSA levels during the course of therapy. No such correlation could be determined for bone density measurements of metastatic bone lesions. Compared to the fully diagnostic CT scan, a significantly higher proportion of bone metastases was detected on ^{68}Ga-PSMA-11 PET.

Keywords ^{68}Ga-PSMA-11 PET/CT · Quantitative tumor parameters · Bone metastases · Treatment response

Introduction

Bone metastases are a frequent complication of cancer occurring in up to 30% of patients with prostate cancer (PC) [1]. The presence of bone metastases in PC patients

✉ Christian Schmidkonz
christian.schmidkonz@uk-erlangen.de

Extended author information available on the last page of the article

has a considerable effect not only on morbidity including complications like pain, pathologic fractures, disability, spinal cord or nerve root compression, and marrow infiltration, but also on mortality, since unlike deaths from many other types of cancer and deaths from PC are often due to advanced bone disease [2, 3]. Early detection of bone metastases is, therefore, pivotal for accurate staging, choice of optimal treatment strategies, and therapeutic monitoring. In recent years, molecular hybrid imaging using small molecule inhibitors targeting the prostate-specific membrane antigen (PSMA) is increasingly used for staging and restaging in prostate cancer [4].

Currently, response assessment in PC is based on changes of the prostate-specific antigen (PSA) serum levels and on the evaluation of computed tomography (CT) or magnetic resonance imaging (MRI) using the response evaluation criteria in solid tumors (RECIST) in their current version 1.1 [5] and other clinical outcome parameters [6]. However, in bone metastases, the revised RECIST 1.1 criteria are of limited use, since osteoblastic metastases, the most common type in patients with prostate cancer [7], are considered immeasurable. Furthermore, for osteoblastic lesions an increase in density is seen in both, progressing and responding disease, hampering visual evaluation of response to therapy [8].

Quantitative evaluation of bone metastases using ^{68}Ga-PSMA-11 PET/CT—demonstrating PSMA uptake in the sclerotic lesion representing the presence of vital tumor cells—might become an important method to determine therapeutic response or progression of skeletal disease in prostate cancer patients. However, for determination of overall response to therapy, individual lesion standard uptake values (SUV) measurements might be inadequate. Therefore, a parameter reflecting the whole-body tumor burden based on the volume, the number, and the PSMA expression of tumor lesions is urgently needed. To the best of our knowledge, the concept of whole-body tumor burden in patients with prostate cancer has so far only been addressed in the study of Schmuck et al. [9] and in a recently published paper by our group [10]. It has, as yet, neither been studied how relevant the additional morphologic information of a fully diagnostic CT scan of ^{68}Ga-PSMA-11 PET/CT is, nor if the concept of whole-body tumor burden is applicable in patients with biochemical recurrence of PC suffering from bone metastases. Therefore, the aim of this study was to compare ^{68}Ga-PSMA-11 PET findings with fully diagnostic CT findings by including all bone lesions in the FOV for calculation of quantitative volumetric tumor parameters as well as to compare PET findings with biochemical evaluations in a small group of patients who underwent ^{68}Ga-PSMA-11 PET at two time points for assessment of therapeutic response.

Methods

Patients

A total of 177 men who were referred due to biochemical recurrence of prostate cancer were retrospectively included in this study.

Patients were selected according to the following inclusion criteria:

- Histopathologically confirmed PC.
- Completed primary therapy (prostatectomy with or without lymph-node dissection or radiotherapy, optionally combined with androgen deprivation therapy).
- Biochemical recurrence of prostate cancer.
- Available clinical history including Gleason score and PSA level at time of PET/CT.
- At least one PSMA-positive bone lesion on the ^{68}Ga-PSMA-11 PET/CT scan.

The diagnosis of biochemically recurrent disease was carried out by the referring urologist and was based on the criteria outlined in the European Association of Urology (EAU) guidelines on Prostate Cancer [11, 12].

A total of 20 patients suffering from bone metastases only, which were also retrospectively identified, underwent ^{68}Ga-PSMA-ligand PET/CT before initiation and after completion of therapy. Patient characteristics are collected in Tables 1 and 2. All studies were performed in the course of clinical work-up of patients. ^{68}Ga-PSMA-HBED-CC (^{68}Ga-PSMA-11) is an investigational radiopharmaceutical and is not yet approved by the Food and Drug Administration (FDA) or the European Medicines Agency (EMA). It was, therefore, administered under the conditions outlined in §13(2b) of the Arzneimittelgesetz (AMG; German Medicinal Products Act) and in compliance with the Declaration of Helsinki. This retrospective study was performed according to the guidelines of the IRB under the auspices of the Bavarian law concerning hospitals [Bayerisches Krankenhausgesetz 27(4)]. All patients signed a written informed consent form for the purpose of anonymized evaluation and publication of their data.

Radiosynthesis and formulation of 68Ga-PSMA-HBED-CC (68Ga-PSMA-11)

The radiosynthesis of Glu-NH-CO–NH-Lys-(Ahx)-[68Ga(HBED-CC)] (68Ga-PSMA-HBED-CC or ^{68}Ga-PSMA-11) was performed under clean room conditions in a GMP-compliant manner, following the procedure

Table 1 Patient characteristics of the entire study population

Parameter	Value
Patient number	177
^{68}Ga-PSMA-11-positive bone lesions	443
Age	
Mean ± SD	70 ± 4 years
Range	54–85 years
Primary Treatment	
Radical prostatectomy	74
Radical prostatectomy + adjuvant radiotherapy	71
Primary radiotherapy	32
Primary Gleason Score	
Gleason 6	11
Gleason 7	48
Gleason 8	47
Gleason 9	68
Gleason 10	3
Median	8
Range	6–10
ADT (%)	
Present	40
Absent	137
PSA (ng/ml)	
Mean ± SD	8.2 ± 16.0
Range	0.1–150.0

Table 2 Patient characteristics of patients who underwent baseline and follow-up ^{68}Ga-PSMA-11 PET/CT

Parameter	Value
Patient number	20
^{68}Ga-PSMA-11-positive lesions	173
Age	
Mean ± SD	71 ± 9 years
Range	54–90 years
Primary treatment	
Radical prostatectomy	5
Radical prostatectomy + adjuvant radiotherapy	10
Primary radiotherapy	5
Primary Gleason Score	
Median	8
Range	7–9
Treatment after first ^{68}Ga-PSMA-11 PET/CT	
Radiation therapy	13
Androgen deprivation therapy	4
Chemotherapy	2
^{177}Lu-PSMA peptide radionuclide therapy	1
ADT (%)	
Present	12
Absent	8
PSA (ng/ml)	
Mean ± SD	13.2 ± 32.7
Range	0.6–150

previously described by Kopka et al. [13], with only slight modifications. The 68Ge/^{68}Ga radionuclide pharmacy grade generator (1850 MBq, GalliaPharmTM, Eckert & Ziegler AG, Berlin, Germany) connected to a Scintomics GRP module (Scintomics GmbH, Fuerstenfeldbruck, Germany), was operated under grade B clean room conditions. 68Ga3+ was prepurified by the use of a cation-exchange cartridge. The final formulation of ^{68}Ga-PSMA-11 was done using isotonic phosphate-buffered saline (PBS) containing not more than 10% ethanol and sterile filtration of 14.5 mL. The mean radioactivity yield of ^{68}Ga-PSMA-11 was 55% (referred to the eluted 68Ga3+) and the radiochemical purity was > 96% as determined by radio-HPLC (Chromolith Performance RP-18e, 100 × 4.6 mm, 5% acetonitrile (0.1% TFA) (up to 0.5 min), 5–80% acetonitrile (0.1% TFA) (0.5–10 min), 2 mL/min, 280 nm). After quality control of ^{68}Ga-PSMA-11, the final solution was approved for administration to patients via intravenous bolus injection.

Imaging procedure

^{68}Ga-PSMA-11 PET/CT imaging was performed using a dedicated PET/CT system (Biograph mCT scanner, Siemens Medical Solutions).

A fully diagnostic, contrast-enhanced CT scan (120 kV, 170 mAs, 16 × 1.2 mm slice collimation, 0.5 s rotation time, pitch 1, reconstructed with filtered backprojection using B30f and B70f kernels, slice thickness 1.5 mm, and increment 1 mm) was performed at a mean of 56 min (range 51–64 min) post-injection (p.i.) of ^{68}Ga-PSMA-11 in a mean radioactivity of 131 ± 29 MBq. Immediately after CT scanning, a whole-body PET scan (skull base to mid-thighs) was acquired (3 min per bed, axial field-of-view of 21.8 cm per bed). The PET data were corrected for random and scattered coincidences, as well as for decay during scanning. PET data were corrected for attenuation using the CT and reconstructed with an ordered subset expectation maximization (OSEM) algorithm with 2 iterations/12 subsets and point-spread-function modelling (Siemens TrueX). All corrections and reconstructions were carried out using the manufacturer's software available on the PET/CT system.

Image analysis

All PET/CT datasets were analyzed with commercially available software (Syngo.via, Siemens Molecular Imaging, Hoffman Estates, IL), allowing review of PET, CT, and fused imaging data. Visual evaluation was performed

by two experienced nuclear medicine physicians and one board-certified radiologist. Diagnostic decisions were made by consensus. A ^{68}Ga-PSMA-11-positive bone lesion was considered suspicious for metastasis if the SUV was higher than the respective normal region (gluteal muscle/lumbar vertebral body). Findings on ^{68}Ga-PSMA-11 PET were correlated with the fused fully diagnostic CT scan. Lesion classification was based on the CT findings of PET-positive bone metastases that were visually classified as either osteoblastic, osteolytic, or mixed by comparing the lesion to adjacent normal bone [14]. Bone lesions without ^{68}Ga-PSMA-11 uptake that were morphologically compatible with benign lesions, e.g., enostosis or hemangioma, were not included in the analysis. For semiquantitative evaluation in all suspected ^{68}Ga-PSMA-11-positive bone lesions ($n=443$), the SUVmean, SUVmax, as well as the PSMA-tumor volume (PSMA-TV) of each lesion were determined in volumes of interest (VOI) with iso-contour set at 45% of the maximum uptake within the respective focus. For each bone lesion, the ^{68}Ga-PSMA-11 uptake was calculated by multiplying the respective PSMA-tumor volume and mean SUV (see Fig. 1 for a representative example). According to previously conducted studies [9, 10], this parameter is called total-lesion PSMA (TL-PSMA). In addition, the diameter of bone metastases was assessed in the axial and sagittal planes to calculate the volume of lesions assuming an elliptic shape. By drawing a two-dimensional region of interest (ROI) surrounding each metastasis, the respective mean Hounsfield Units (HU) were determined (see Fig. 1). Quantitative parameters of all PET-positive/CT-negative (PET+/CT−) bone lesions were compared to the respective parameters in patients with both PET-positive and CT-positive (PET+/CT+) bone lesions.

Response to treatment analysis

In 20 patients, suffering from bone metastases only, that underwent ^{68}Ga-PSMA-11 PET/CT before and after completion of therapy, summation of the PSMA-TV over all lesions of a patient resulted in the whole-body PSMA-TV (wbPSMA-TV) and summation of the TL-PSMA—over all lesions of patient in the whole-body TL-PSMA (wbTL-PSMA). Feasibility of therapy response assessment was evaluated by comparing these parameters to biochemical response based on the change of PSA-serum levels and to changes of HU units of the respective bone lesions following therapy.

Statistical analysis

Descriptive statistics were computed for continuous and categorical variables, including mean, standard deviations (SD), and range for continuous variables, and absolute and relative frequencies for categorical variables. Correlation between ^{68}Ga-PSMA-11 PET-derived parameters, CT-derived parameters, and PSA levels were analyzed using Pearson's rank correlation. Differences between two groups were evaluated using a Wilcoxon rank-sum test. A one-way analysis of variance was used to evaluate whether

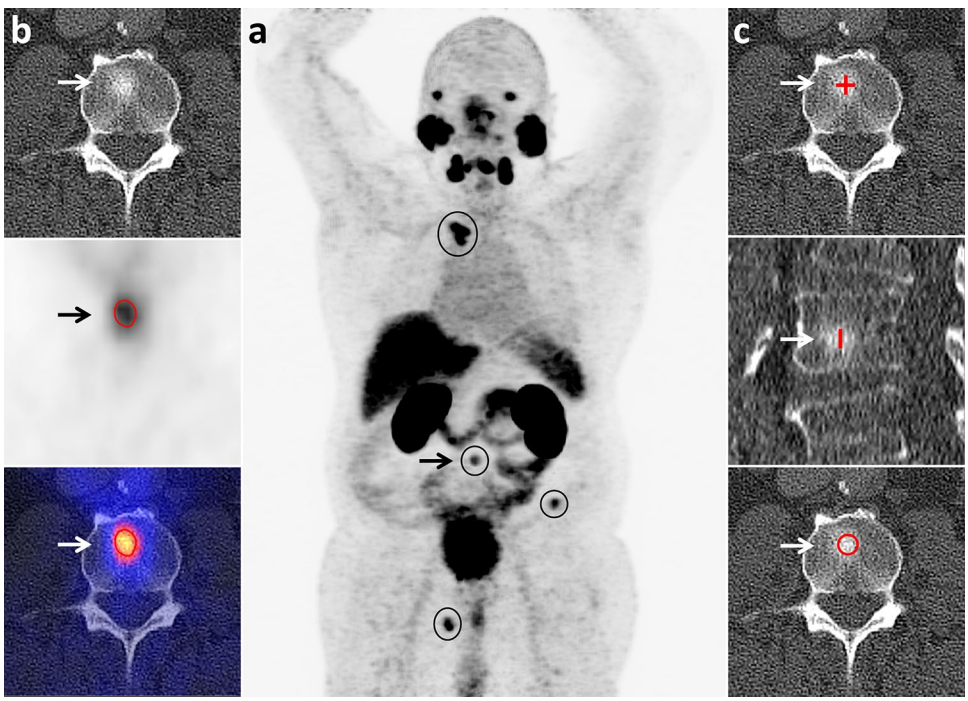

Fig. 1 Assessment of whole-body tumor burden in a 70-year-old patient, Gleason 8 tumor, serum-PSA at examination 19 ng/ml suffering from multiple bone metastases. In the maximum intensity projection: **a** ^{68}Ga-PSMA-11-positive bone lesions are indicated by circles. The left panel **b** demonstrates the segmentation of an osteoblastic lumbar vertebral body metastasis (indicated by arrows) to determinate tumor volume and intensity of tracer uptake for calculation of PSMA-TV and TL-PSMA. CT-derived volumetric assessment of the same metastasis in the axial and sagittal planes and bone density measurement by manual ROI setting are shown in the right panel **c**

SUVmax, SUVmean, wbPSMA-TV, and wbTL-PSMA were different for the patient groups Gleason score ≤ 7 and Gleason > 7. Linear regression analysis was performed to identify dependence between ^{68}Ga-PSMA-11 PET-derived quantitative parameters and biochemical, histological, and CT-derived parameters. For all analyses, a p value < 0.05 was considered statistically significant. Statistical analyses were performed using Matlab version R2012b (The Math Works Inc., Natick, MA).

Results

Descriptive statistics

In 177 patients, a total of 443 bone metastases could be detected on ^{68}Ga-PSMA-11 PET. Of these, 50 PSMA-positive bone lesions (11%) in 21 patients were only visible on ^{68}Ga-PSMA-11 PET but not on CT (see Fig. 2 for a representative example). Of the remaining 393 bone lesions, 331 were rated as osteoblastic (84%), 32 as mixed (8%), and 30 as osteolytic (8%).

Comparison of Gleason Scores with PET parameters and CT-derived measurements

SUVmax, SUVmean, PSMA-TV, and TL-PSMA of bone metastases were significantly higher ($p < 0.05$) in patients with Gleason Scores > 7 compared to those with Gleason Scores ≤ 7. 32 as mixed (8%) and 30 as osteolytic (8%). Osteoblastic metastases demonstrated significantly higher mean HU values compared to mixed and osteolytic metastases, while osteolytic metastases demonstrated a higher CT-derived volume compared to osteoblastic and mixed metastases (Table 3). There was no significant correlation

Table 3 Bone density measurements (HU) and CT-derived volume of osteoblastic-, mixed-, and osteolytic bone lesions

	Osteoblastic	Mixed	Osteolytic
HU	630.9 ± 151.8	247.6 ± 169.2	115.5 ± 79.9
CT-derived volume (cm^3)	3.6 ± 4.3	4.2 ± 5.2	5.3 ± 6.8
Number of lesions	331	32	30

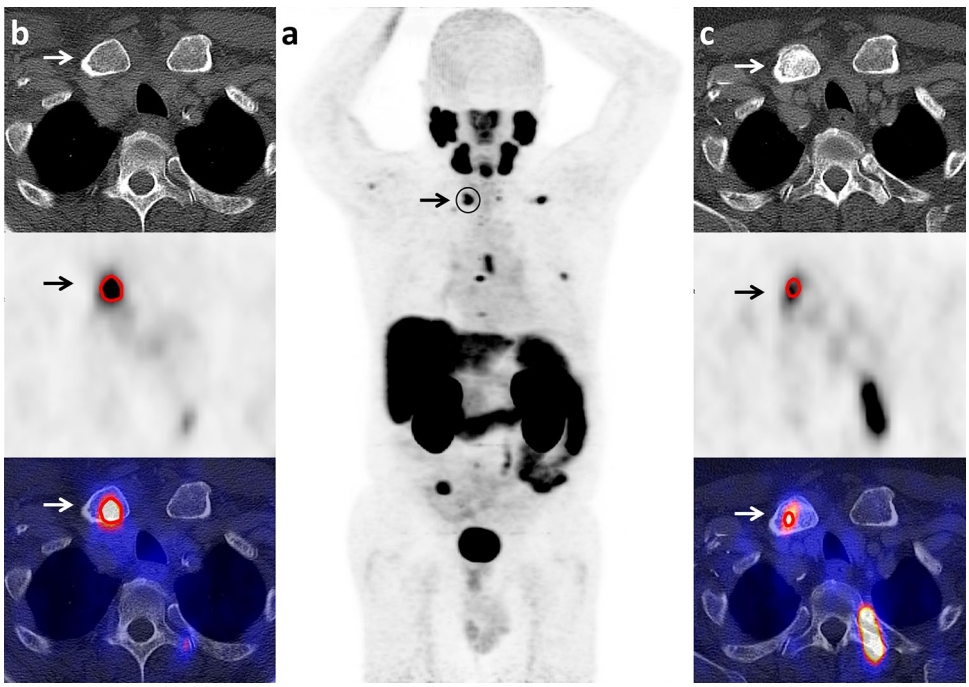

Fig. 2 ^{68}Ga-PSMA-11 PET/CT-derived quantitative volumetric tumor parameters for assessment of therapeutic response in a 63-year-old patient, Gleason 9 tumor, and serum-PSA at first examination of 14 ng/ml. Maximum intensity projection **a** demonstrates a ^{68}Ga-PSMA-11-positive bone lesion in the right clavicular (indicated by circle and arrow) clearly visible on the corresponding PET image **b**. The corresponding CT image at the same level shows no respective morphological alteration. In the follow-up PET/CT 6 months after initiation of androgen deprivation therapy, conventional CT shows an osteoblastic lesion **c** at the site of the former tracer accumulation. Serum PSA decreased to 3.5 ng/ml. The corresponding PET image shows partial remission of the previous tracer accumulation. PSMA-TV and TL-PSMA decreased concordantly

of ^{68}Ga-PSMA-11 PET parameters nor of Gleason Scores with mean HU values of bone lesions (Fig. 3).

Quantitative evaluation of all 393 bone metastases visible on both PET and CT yielded the highest SUVmax, SUVmean as well as the highest TL-PSMA values for mixed lesions, while osteolytic lesions showed the highest PSMA-TV. All three types of bone lesions demonstrated a significant correlation between PSMA-TV and the CT-derived volumetric measurements ($r = 0.47$, $p < 0.001$). Results are summarized in Table 4.

The dependence between the SUVmean of PET-positive bone metastases and the variables Gleason Score, CT-derived bone density (measured in Hounsfield units), lesion classification (based on the visual evaluation of metastatic lesions and comparison to adjacent normal bone), and serum-PSA level was investigated in the linear regression model.

The model gives a p value < 0.01, which means that the chosen parameters are sufficient to model the SUVmean. A significant association was determined between SUVmean, Gleason Scores, lesion classification, and serum-PSA levels. Higher SUVmean values were associated with higher Gleason Scores, higher serum-PSA levels and mixed lesions. Bone metastases in patients with Gleason Scores of 9 were associated with higher SUVmean values compared to patients with Gleason Scores of 8.

Comparison of ^{68}Ga-PSMA-11-PET-derived parameters in patients with PET-positive/CT-negative bone metastases (PET+/CT−) in contrast to patients with PET-positive/CT-positive (PET+/CT+) bone metastases

Quantitative PET parameters of the 50 ^{68}Ga-PSMA-11 PET+/CT− bone metastases in 21 patients were compared to the 393 PET+/CT+ bone metastases in 156 patients. SUVmax, SUVmean, and TL-PSMA values of PET+/CT− were significantly lower (Wilcoxon rank-sum test, all $p < 0.05$) compared to PET+/CT+ bone metastases, while no significant difference was found for PSMA-TV between both groups (Wilcoxon rank-sum test, $p = 0.83$) (Fig. 4).

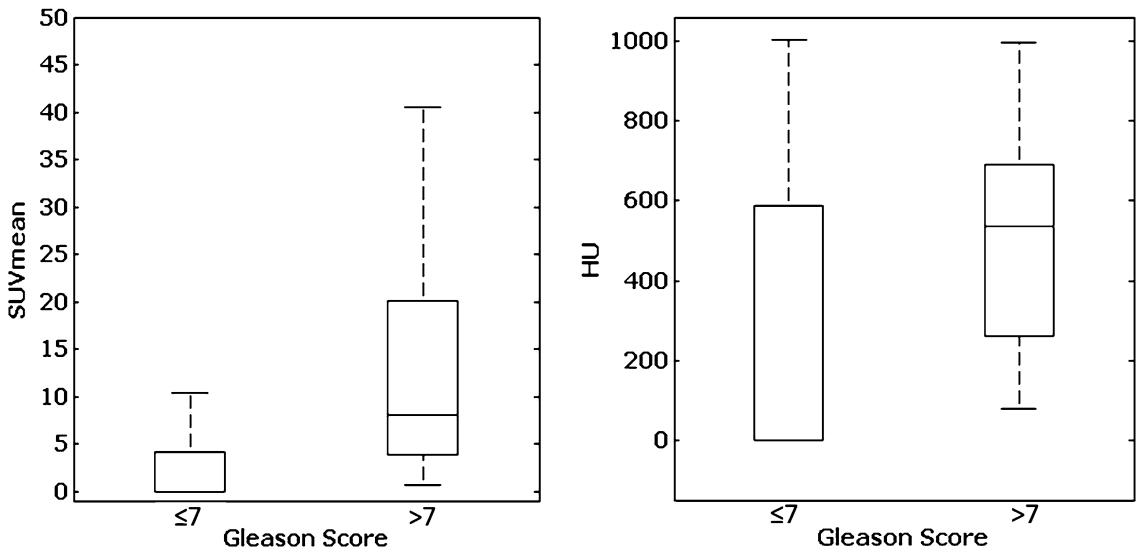

Fig. 3 Ga-PSMA-11 PET-derived quantitative tumor parameters, e.g., SUVmean, were significantly higher in prostate cancer patients with a Gleason Score of 7 or higher than compared to patients with a Gleason Score of 7 or below that threshold. No such correlation could be found between bone density measurements (HU) and Gleason Scores

Table 4 Mean, standard deviation, and 95% confidence intervals of the respective PET parameters and the corresponding lesion type in 393 bone metastases visible on PET and CT

	Osteoblastic	Mixed	Osteolytic
SUVmax	19.9 ± 24.2 (16.7–23.1)	21.9 ± 28.5 (10.9–33.0)	16.7 ± 17.3 (10.2–23.1)
SUVmean	13.4 ± 16.1 (11.3–15.5)	14.7 ± 18.6 (7.5–21.9)	10.9 ± 11.2 (6.7–15.1)
PSMA-TV	1.5 ± 2.0 (1.3–1.9)	1.2 ± 1.8 (0.7–3.4)	2.8 ± 3.4 (1.1–3.5)
TL-PSMA	18.6 ± 42.1 (13.1–24.2)	42.1 ± 122.9 (5.5–89.8)	28.0 ± 57.3 (6.6–49.4)

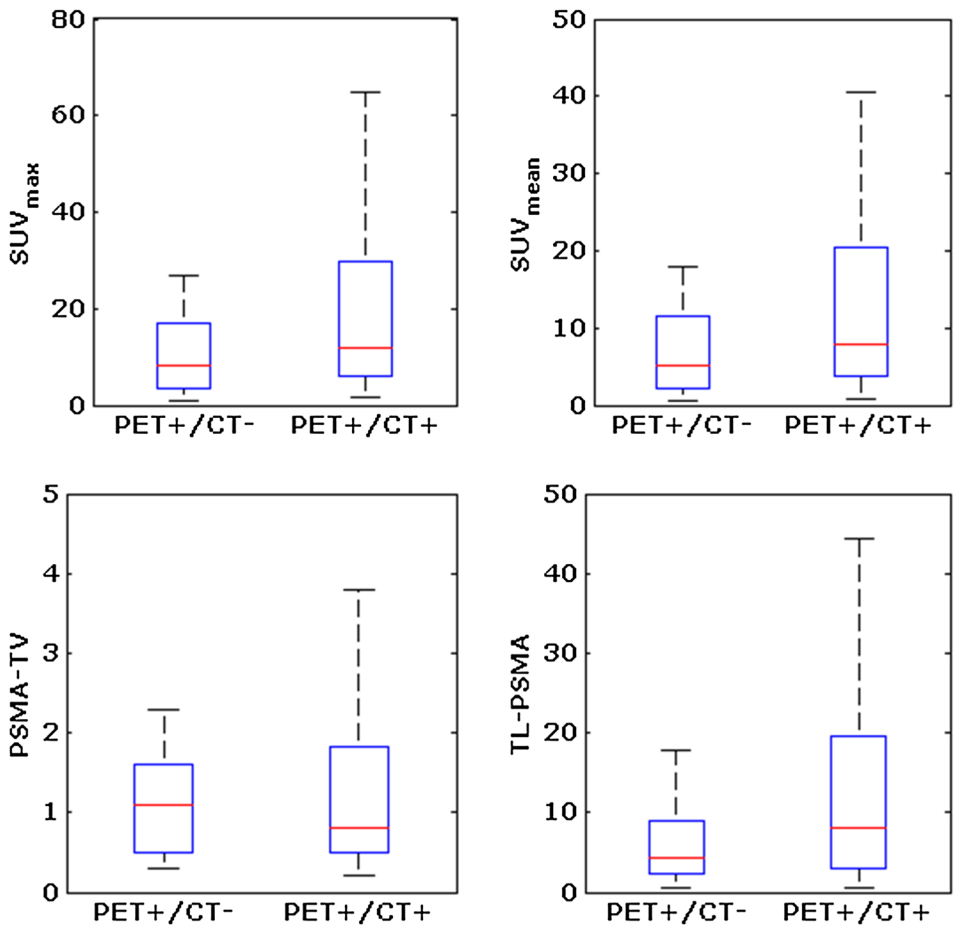

Fig. 4 Comparative analysis of quantitative ^{68}Ga-PSMA-11 PET-derived quantitative tumor parameters between PET-positive/CT-negative (PET + /CT-) and PET-positive/CT-positive (PET + /CT +) bone metastases

Therapeutic response evaluation using ^{68}Ga-PSMA-11 PET-, biochemical-, and CT-derived parameters

A total of 20 patients suffering from 173 bone metastases underwent ^{68}Ga-PSMA-11 PET/CT imaging before and after therapies, and were retrospectively included in the therapeutic response evaluation. The study cohort consisted of 12 patients who underwent external beam radiation therapy, 5 patients who underwent androgen deprivation therapy, 2 patients who underwent docetaxel chemotherapy, and 1 patient who underwent ^{177}Lu-PSMA-617 radionuclide therapy.

Bone metastases showed a mean density of 589 ± 203 HU before therapy with a significant increase to 827 ± 215 HU ($p < 0.05$) after therapy. However, no significant changes of CT-derived volumetric measurements before and after therapies were observed ($p > 0.05$). Furthermore, there was no significant correlation between the percentage differences of CT-derived HU-values and serum-PSA levels ($\rho = 0.01$, $p = 0.97$) and CT-derived volumetric measurements and serum-PSA levels ($\rho = -0.15$, $p = 0.53$) before and after therapies.

In contrast, a significant correlation was observed between the percentage difference of whole-body PSMA-TV and the percentage difference of serum-PSA levels ($\rho = 0.98$, $p < 0.001$) (Fig. 5) as well as for the percentage difference of whole-body TL-PSMA and the percentage difference of serum-PSA levels ($\rho = 0.93$, $p < 0.001$) (Fig. 6) before and after therapies. PSMA-TV and TL-PSMA increased in all

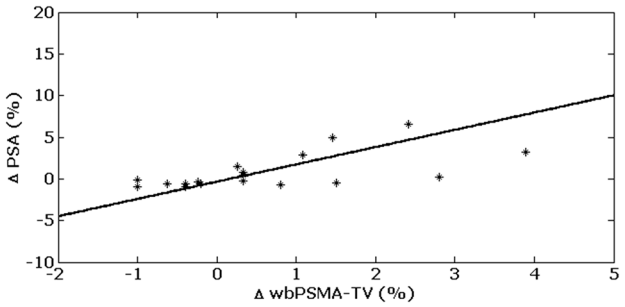

Fig. 5 Percentage differences of whole-body PSMA-TV (Δ wbPSMA-TV) demonstrate a significant correlation ($\rho = 0.98$, $p < 0.001$) with percentage differences of serum-PSA levels (Δ PSA)

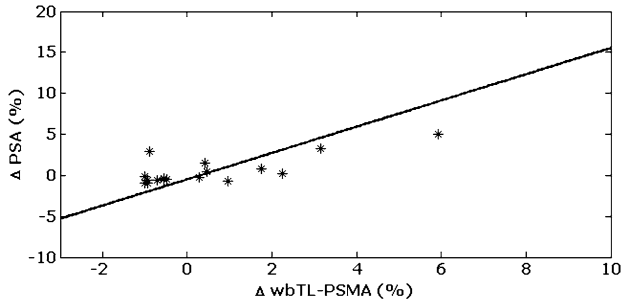

Fig. 6 Percentage differences of whole-body TL-PSMA (Δ wbTL-PSMA) correlate significantly ($\rho = 0.93$, $p < 0.001$) with percentage differences of serum-PSA levels (Δ PSA)

patients with rising PSA-serum levels and decreased in all patients with decreasing PSA-serum levels.

Discussion

This is the first study that evaluated the capability of ^{68}Ga-PSMA-11 PET/CT-derived quantitative volumetric tumor parameters for classification and determination of response to therapy of bone metastases in comparison with fully diagnostic conventional CT in patients with metastasized prostate cancer. In our study cohort, a total of 443 PSMA-positive bone lesions were detected of which 50 bone metastases (11%) were not visible on the fully diagnostic CT scan. A previously conducted study by Sachpedkidis et al. [15] compared ^{68}Ga-PSMA-11 PET findings and low-dose CT findings in a heterogeneous group of prostate cancer patients suffering from biochemical recurrence. A total of 168 ^{68}Ga-PSMA-11 PET-positive bone lesions were detected of which 65 bone metastases (39%) were not visible in the low-dose CT. The large discrepancy between these findings suggest that a fully diagnostic CT scan demonstrates a significant higher proportion of morphologic bone changes suggestive for metastasis and might reduce the rate of unequivocal findings of PSMA-positive bone lesions without a CT-morphological correlate. The comparative quantitative subgroup analysis between ^{68}Ga-PSMA-11 PET + /CT- bone metastases and ^{68}Ga-PSMA-11 PET + /CT + bone metastases demonstrated significant lower SUVmax, SUVmean, and TL-PSMA values for PET+/CT− bone metastases, while no significant difference was observed for PSMA-TV values. A possible explanation for this might be that ^{68}Ga-PSMA-11 PET detects metabolic changes in bone tissue during the development of bone metastases in a very early stage, when PSMA expression is still low and morphologic changes to healthy bone tissue are not yet detectable. In later stages of metastatic bone disease, PSMA expression increases due to higher tumor aggressiveness [16] and the destruction of healthy bone tissue becomes visible on conventional CT.

In addition, we found that SUVmax, SUVmean, PSMA-TV, and TL-PSMA of bone metastases were significantly higher in patients with primary Gleason Scores of > 7 compared to lower Gleason Scores, while there was no such correlation between Gleason Scores and HU. In the linear regression analysis, all types of bone metastases in patients with Gleason Scores of 9 demonstrated higher SUVmean values compared to patients with Gleason Score 8; again, no such correlation could be determined for bone density measurements. The explanation for this might be that PET parameters take into account the degree of PSMA expression on tumor cells which is regularly elevated at higher Gleason Scores [17, 18]. Quantitative analysis of the different type of bone lesions yielded a trend towards higher tracer uptake of mixed lesions, while osteolytic lesions demonstrated the highest tumor volume; however, the differences did not reach statistical significance. In contrast to our results, Jannsen et al. [19] found the highest SUVmax values in osteolytic metastases followed by mixed and osteoblastic lesions. The differences between their results and ours might be due the higher patient number and the higher number of bone lesions which were evaluated in our study. Interestingly, the CT-derived volumetric measurements for osteoblastic, mixed, and osteolytic lesions correlated significantly with PSMA-TV, which was not the case in the study by Jannsen and colleagues.

Since osteoblastic metastases are the most common type of bone metastases in prostate cancer, and bone metastases without a soft-tissue component > 10 mm are considered immeasurable by the RECIST 1.1 criteria [5], assessment of response to therapy by the conventional CT is limited. Sclerosis of a lytic component on CT suggests response to treatment [14] and can be interpreted visually or by measuring the bone density in Hounsfield Units during the course of therapy. Recently conducted studies [10, 20] concluded that assessment of response to therapy using ^{68}Ga-PSMA-11 PET-derived quantitative tumor parameters shows higher concordance with biochemical response evaluation based on serum-PSA levels that are an integral part of current recommendations for therapy response assessment in advanced prostate cancer [21] compared to the conventional CT. Foerster et al. [22] retrospectively assessed osteolytic metastases in breast cancer patients and found a significant increase of bone density following external beam radiation therapy. Since there are no data regarding the change of bone density of osteolytic-, mixed-, and osteoblastic bone metastases in prostate cancer patients following different therapy regimens, we could demonstrate that all three types of PSMA-positive bone lesions demonstrated a significant increase of bone density suggestive for response to therapy. Interestingly, we did not observe a correlation between

the mean differences of Hounsfield units and CT-derived volumetric measurements of bone metastases and the percentage difference of serum-PSA levels in the baseline and follow-up examination. In contrast, the mean differences of PSMA-TV and TL-PSMA reflecting the total tumor load of patients showed a highly significant correlation with changes of serum-PSA levels. However, despite the good correlation with quantitative tumor markers derived from ^{68}Ga-PSMA-11 PET, PSA alone might not be sufficiently reliable for assessment of treatment response in all cases. Since conventional CT and PSA levels are limited in the evaluation of response to therapy in bone metastases, especially if they lack a soft-tissue component and are, therefore, considered immeasurable according to RECIST 1.1 ^{68}Ga-PSMA-11 PET/CT might be of additional value. Quantification of PSMA expression of bone metastases during the course of therapy enables the early detection of tumor progression or response to therapy and might support the treating physician in the decision if change of further therapy is necessary. The determination of not only the established SUVmax and SUVmean parameters that characterize the intensity of tracer uptake in individual tumor lesions but also PSMA-TV and TL-PSMA might further improve the assessment of response to therapy. PSMA-TV describes the metabolic active tumor volume of a PSMA-positive lesion, while TL-PSMA takes into account not only the metabolic active tumor volume but also the metabolic activity of tumor lesions, and enables the assessment of whole-body tumor burden that might allow the better stratification of patients into low- and high-volume metastatic disease.

A PSA flare (temporary increase) is described in up to 13% of patients under docetaxel chemotherapy [23] and in up to 11% of patients under androgen deprivation therapy [13], and might lead to a misclassification of therapeutic response. This phenomenon was also described previously for ^{68}Ga-PSMA-11 PET/CT [24]. Early increases of PSMA uptake in metastatic tumor lesions, after initiation of androgen deprivation therapy, that were indicative of a flare effect rather than disease progression were observed in patients that subsequently achieved PSA declines of > 50% from baseline and, therefore, have to be interpreted with caution. Focal PSMA uptake in the skeleton is usually considered to indicate the presence of bone metastases unless it can be attributed to a corresponding skeletal lesion. However, PSMA uptake can be found in a variety of benign bone lesions, e.g., Paget disease, healing fractures, and degenerative arthritis [25]. Comparison with morphological findings on the CT component are, therefore, of utmost importance. Furthermore, the occurrence of PET-positive/CT-negative has to be interpreted with caution, since it might be possible that in an early stage of benign bone changes, there is already an increased PSMA uptake without a morphological correlate in the conventional CT.

Altogether, our results suggest a possible role of ^{68}Ga-PSMA-11 PET-derived quantitative volumetric tumor parameters for evaluation of therapeutic response of bone metastases in prostate cancer patients.

Limitations

Our study suffers from several limitations. First, the retrospective nature of this single-center study has typical limitations. Possible biases from patient referrals and treatments cannot be excluded. Histological confirmation as a gold standard of each PSMA-positive bone metastasis would have been preferable, but was not feasible. It cannot be excluded that a PSA flare and also a flare phenomenon in PSMA PET/CT under androgen deprivation therapy might have been occurred in some of the patients that were included in our study.

Unfortunately, only 20 patients suffering from bone metastases only that underwent different treatment regimens underwent baseline and follow-up ^{68}Ga-PSMA-11 PET/CT for therapeutic response evaluation. These preliminary but nevertheless interesting results may support the hypothesis that hybrid PSMA imaging may enhance diagnostic performance and also provide higher accuracy in response assessment in prostate cancer patients suffering from bone metastases. To determine the validity of ^{68}Ga-PSMA-11 PET/CT-derived quantitative volumetric tumor parameters for evaluation of bone metastases from prostate cancer long-term follow-up and survival in treated patients have to be evaluated in larger prospective multicentre trials.

Conclusion

Our results suggest that ^{68}Ga-PSMA-11 PET/CT might be a valuable tool for the detection and follow-up of bone metastases in patients with metastasized prostate cancer. ^{68}Ga-PSMA-11 PET-derived quantitative volumetric parameters demonstrated a highly significant correlation with changes of serum-PSA levels during the course of therapy. No such correlation could be determined for bone density measurements of metastatic bone lesions. Compared to the fully diagnostic CT scan, a significantly higher proportion of bone metastases was detected on ^{68}Ga-PSMA-11 PET.

References

1. Hernandez RK, Wade SW, Reich A, Pirolli M, Liede A, Lyman GH. Incidence of bone metastases in patients with solid tumors: analysis of oncology electronic medical records in the United States. BMC Cancer. 2018;18(1):44.
2. Bäuerle T, Semmler W. Imaging response to systemic therapy for bone metastases. Eur Radiol. 2009;19(10):2495–507.

3. Lange PH, Vessella RL. Mechanisms, hypotheses and questions regarding prostate cancer micrometastases to bone. Cancer Metastasis Rev. 1998;17(4):331–6.
4. Afshar-Oromieh A, Babich JW, Kratochwil C, Giesel FL, Eisenhut M, Kopka K, et al. The rise of PSMA ligands for diagnosis and therapy of prostate cancer. J Nucl Med. 2016;57(Supplement 3):79S–89S.
5. Eisenhauer E, Therasse P, Bogaerts J, Schwartz L, Sargent D, Ford R, et al. New response evaluation criteria in solid tumours: revised RECIST guideline (version 1.1). Eur J Cancer. 2009;45(2):228–47.
6. Thalgott M, Rack B, Eiber M, Souvatzoglou M, Heck MM, Kronester C, et al. Categorical versus continuous circulating tumor cell enumeration as early surrogate marker for therapy response and prognosis during docetaxel therapy in metastatic prostate cancer patients. BMC Cancer. 2015;15(1):458.
7. Mundy GR. Metastasis: Metastasis to bone: causes, consequences and therapeutic opportunities. Nat Rev Cancer. 2002;2(8):584.
8. Vinholes J, Coleman R, Eastell R. Effects of bone metastases on bone metabolism: implications for diagnosis, imaging and assessment of response to cancer treatment. Cancer Treat Rev. 1996;22(4):289–331.
9. Schmuck S, von Klot CA, Henkenberens C, Sohns JM, Christiansen H, Wester H-J, et al. Initial experience with volumetric 68Ga-PSMA I&T PET/CT for assessment of whole-body tumor burden as a quantitative imaging biomarker in patients with prostate cancer. J Nucl Med. 2017;58(12):1962–8.
10. Schmidkonz C, Cordes M, Schmidt D, Bäuerle T, Goetz TI, Beck M, et al. ^{68}Ga-PSMA-11 PET/CT-derived metabolic parameters for determination of whole-body tumor burden and treatment response in prostate cancer. Eur J Nucl Med Mol Imaging. 2018:1–11.
11. Heidenreich A, Bastian PJ, Bellmunt J, Bolla M, Joniau S, van der Kwast T, et al. EAU guidelines on prostate cancer. Part 1: screening, diagnosis, and local treatment with curative intent—update 2013. Eur Urol. 2014;65(1):124–37.
12. Cornford P, Bellmunt J, Bolla M, Briers E, De Santis M, Gross T, et al. EAU-ESTRO-SIOG guidelines on prostate cancer. Part II: treatment of relapsing, metastatic, and castration-resistant prostate cancer. Eur Urol. 2017;71(4):630–42.
13. Burgio SL, Conteduca V, Rudnas B, Carrozza F, Campadelli E, Bianchi E, et al. PSA flare with abiraterone in patients with metastatic castration-resistant prostate cancer. Clin Genitourin Cancer. 2015;13(1):39–433.
14. Hamaoka T, Madewell JE, Podoloff DA, Hortobagyi GN, Ueno NT. Bone imaging in metastatic breast cancer. J Clin Oncol. 2004;22(14):2942–53.
15. Sachpekidis C, Bäumer P, Kopka K, Hadaschik B, Hohenfellner M, Kopp-Schneider A, et al. ^{68}Ga-PSMA PET/CT in the evaluation of bone metastases in prostate cancer. Eur J Nucl Med Mol Imaging. 2018;45:904–12.
16. Ross JS, Sheehan CE, Fisher HA, Kaufman RP, Kaur P, Gray K, et al. Correlation of primary tumor prostate-specific membrane antigen expression with disease recurrence in prostate cancer. Clin Cancer Res. 2003;9(17):6357–62.
17. Kasperzyk JL, Finn SP, Flavin RJ, Fiorentino M, Lis RT, Hendrickson WK, et al. Prostate-specific membrane antigen protein expression in tumor tissue and risk of lethal prostate cancer. Cancer Epidemiol Biomarkers Prev. 2013;22:2354–63.
18. Marchal C, Redondo M, Padilla M, Caballero J, Rodrigo I, Garcia J, et al. Expression of prostate specific membrane antigen (PSMA) in prostatic adenocarcinoma and prostatic intraepithelial neoplasia. Histol Histopathol. 2004;19:715–8.
19. Janssen J-C, Woythal N, Meißner S, Prasad V, Brenner W, Diederichs G, et al. [68Ga] PSMA-HBED-CC uptake in osteolytic, osteoblastic, and bone marrow metastases of prostate cancer patients. Mol Imaging Biol. 2017;19(6):933–43.
20. Seitz AK, Rauscher I, Haller B, Krönke M, Luther S, Heck MM, et al. Preliminary results on response assessment using 68Ga-HBED-CC-PSMA PET/CT in patients with metastatic prostate cancer undergoing docetaxel chemotherapy. Eur J Nucl Med Mol Imaging. 2018;45(4):602–12.
21. Scher HI, Morris MJ, Stadler WM, Higano C, Basch E, Fizazi K, et al. Trial design and objectives for castration-resistant prostate cancer: updated recommendations from the Prostate Cancer Clinical Trials Working Group 3. J Clin Oncol. 2016;34(12):1402.
22. Foerster R, Eisele C, Bruckner T, Bostel T, Schlampp I, Wolf R, et al. Bone density as a marker for local response to radiotherapy of spinal bone metastases in women with breast cancer: a retrospective analysis. Radiat Oncol. 2015;10(1):62.
23. Nelius T, Filleur S. PSA surge/flare-up in patients with castration-refractory prostate cancer during the initial phase of chemotherapy. Prostate. 2009;69(16):1802–7.
24. Aggarwal R, Wei X, Kim W, Small EJ, Ryan CJ, Carroll P, et al. Heterogeneous flare in prostate-specific membrane antigen positron emission tomography tracer uptake with initiation of androgen pathway blockade in metastatic prostate cancer. Eur Urol Oncol. 2018;1(1):78–82.
25. Shetty D, Patel D, Le K, Bui C, Mansberg R. Pitfalls in gallium-68 PSMA PET/CT interpretation—a pictorial review. Tomography. 2018;4(4):182.

Affiliations

Christian Schmidkonz[1,5] · Michael Cordes[1] · Theresa Ida Goetz[1,4] · Olaf Prante[1] · Torsten Kuwert[1] · Philipp Ritt[1] · Michael Uder[2] · Bernd Wullich[3] · Peter Goebell[3] · Tobias Bäuerle[2]

1 Department of Nuclear Medicine , Friedrich-Alexander University Erlangen-Nürnberg (FAU) , Erlangen, Germany

2 Institute of Radiology , Friedrich-Alexander University Erlangen-Nürnberg (FAU) , Erlangen, Germany

3 Department of Urology and Pediatric Urology , Friedrich-Alexander University Erlangen-Nürnberg (FAU) , Erlangen, Germany

4 Pattern Recognition Lab , Friedrich-Alexander University Erlangen-Nürnberg (FAU) , Erlangen, Germany

5 Clinic of Nuclear Medicine , University of Erlangen-Nuremberg , Ulmenweg 18, 91054 Erlangen, Germany